

# PROBABILISTIC SEISMIC HAZARD ASSESSMENT OF TEHRAN BASED ON ARIAS INTENSITY

G. Ghodrati Amiri, H. Mahmoodi\* and S.A. Razavian Amrei

Department of Civil Engineering, Iran University of Science and Technology  
P.O. Box 16765-163, Tehran, Iran  
ghodrati@iust.ac.ir – hmd.mahmoodi@gmail.com – ali\_razavian@iust.ac.ir

\*Corresponding Author

(Received: February 23, 2009 – Accepted in Revised Form: November 5, 2009)

**Abstract** A probabilistic seismic hazard assessment in terms of Arias intensity is presented for the city of Tehran. Tehran is the capital and the most populated city of Iran. From economical, political and social points of view, Tehran is the most significant city of Iran. Many destructive earthquakes happened in Iran in the last centuries. Historical references indicate that the old city of Rey and the present Tehran have been destroyed by catastrophic earthquakes at least 6 times. Existence of active faults like North of Tehran, Mousa and North and South of Rey is the main causes of seismicity of this city. Seismicity parameters on the basis of historical and instrumental earthquakes for a time period, from 4th century BC to the present time are calculated using Tavakoli's approach and Kijko method. The earthquake catalogue with a radius of 200 km around Tehran has been used to calculate seismicity parameters. Iso-intensity contour lines maps of Tehran on the basis of different attenuation relationships are plotted. They display the probabilistic estimate of Arias intensity with Rock and Soil beds for the return periods of 72, 224, 475, 2475 years. SEISRISKIII software has been employed for seismic hazard assessment. Effects of different parameters such as seismicity parameters, length of fault rupture relationships, and attenuation relationships are considered using logic tree.

**Keywords** Probabilistic Seismic Hazard, Arias Intensity, Seismicity Parameters, Tehran, Iran

**چکیده** این مقاله به ارزیابی احتمالاتی خطر لرزه‌ای شهر تهران با استفاده از پارامتر شدت Arias می‌پردازد. تهران پایتخت و پرجمعیت‌ترین شهر ایران است و از لحاظ اقتصادی، اجتماعی و سیاسی مهم‌ترین شهر ایران محسوب می‌شود. از نقطه نظر لرزه‌خیزی نیز، با استناد به مراجع تاریخی، شهر قدیم ری و تهران کنونی، ۶ بار توسط زلزله‌های سهمگین ویران شده‌است. وجود گسل‌های فعالی مثل شمال تهران، مشاء، شمال و جنوب ری دلیل اصلی لرزه خیز بودن این شهر است. پارامترهای لرزه‌خیزی بر مبنای زلزله‌های تاریخی و دستگاهی برای یک دوره زمانی که از ۴ قرن پیش از میلاد آغاز می‌شود و تا زمان حاضر ادامه پیدا می‌کند، تعیین شده‌اند. این پارامترها با استفاده از رهیافت توکلی و روش Kijko بدست آمده‌اند. برای محاسبه پارامترهای لرزه‌خیزی از یک کاتالوگ زلزله که زلزله‌های آن تا شعاع ۲۰۰ کیلومتری حول تهران رخ داده‌اند استفاده شده است. نقشه‌های حاوی خطوط هم‌شدت برای شهر تهران با استفاده از روابط کاهندگی مختلف رسم شده‌اند. این نقشه‌ها، مقدار شدت Arias احتمالاتی با توجه به دو بستر خاکی و سنگی برای دوره‌های بازگشت ۷۲، ۲۲۴، ۴۷۵، ۲۴۷۵ سال نشان می‌دهند. از نرم افزار SEISRISKIII برای ارزیابی خطر لرزه‌ای شهر تهران استفاده شده است. تاثیر عوامل گوناگونی مثل پارامترهای لرزه‌خیزی، روابط طول پارگی گسل و روابط کاهندگی در درخت منطقی مورد توجه قرار گرفته است.

## 1. INTRODUCTION

Iran is one of the most seismic countries of the world. It is situated over the Himalayan-Alpied seismic belt and is one of those countries which have lost many human lives and a lot of money due to occurrence of earthquakes. Figure 1 shows recent seismicity of Iran [1]. In this country, a

destructive earthquake occurs every several years due to being situated over a seismic zone. Active faults and volcanic high surface elevations along Himalayan-Alpied earthquake belt characterize the Iranian plateau. According to the earthquake data of Iran, most activities are concentrated along Zagros fold thrust belt in comparison to the central and eastern parts of Iran (Figure 1). Thus several

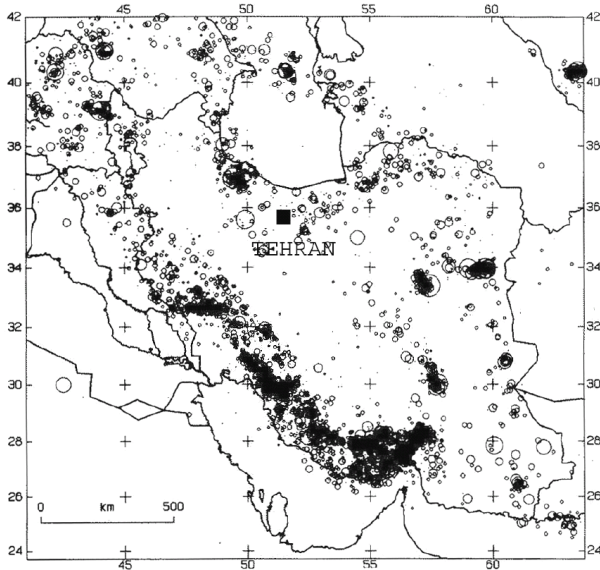


Figure 1. Recent seismicity map of Iran (Ref. [1]).

regions are vulnerable to destructive earthquakes. The seismotectonic conditions of Tehran region are under the influence of the condition of the Iranian tectonic plate in the Middle East.

Tehran as the capital of Iran with the population of over 10 million people is known as an economic and political center. Therefore, destruction in this city has severe effects on the whole country.

Existence of active faults like North of Tehran, Moshfa, North and South of Rey and the past strong earthquakes, indicate the great seismicity of this region and high probability of an earthquake with the magnitude of more than 7. As an example, some strong ground shakings in old Rey city and present Tehran are listed as follows: (Ambraseys, et al [2]):

- 4<sup>th</sup> century BC ( $M_S=7.6$  and  $MMI=X$ )
- 855 AD ( $M_S=7.1$  and  $MMI=VIII$ )
- 958 AD ( $M_S=7.7$  and  $MMI=X$ )
- 1177 AD ( $M_S=7.2$  and  $MMI=VIII$ )
- 1830 ( $M_S=7.1$  and  $MMI=VIII$ )

As stated previously, the presence of active faults in Tehran is the main cause of seismicity of this city. The seismic hazard resulting from an earthquake may include soil liquefaction, landslides, and ground shaking. Ground shaking is considered the most critical seismic hazard, because it affects an extensive area and includes other seismic hazard

such as soil liquefaction (Hwang, et al [3]). Ground motion during earthquake is recorded in the recording stations. Ground motion is affected by many factors such as the characteristics of seismic source, the attenuation of seismic waves from seismic source to recording site and the condition of soil in the recording site. In engineering applications, the ground motion is expressed usually in terms of amplitude, frequency content and the duration of ground motion.

The hazard analysis of Tehran has been performed by Ghodrati Amiri, et al [4] by using the PGA parameter. Since the Arias intensity parameter includes all characteristics of ground motion, it is intended in this paper to perform hazard analysis of Tehran by using Arias intensity. For this purpose, two seismicity relationships, two relationships of fault rupture length and four attenuation relationships associated with Arias intensity will be used by Logic Tree.

As stated above, since Arias intensity includes the entire characteristics of ground motion, it can be very useful in the quantitative estimate of ground motion. Arias intensity will be discussed in comprehensive explanation in the next section.

## 2. ARIAS INTENSITY

The Arias intensity measure (also termed accelerogram energy) is the sum of the energy absorbed by a population of simple oscillators evenly spaced in frequency (Kayen, et al [5]).

Making use of the above definition, some points about Arias intensity are expressed as follows:

- a. Using the above definition and based on a series of simplifications, the Arias intensity formula could be expressed as follows: (Kayen, et al [5]):

$$I_{x-x} = \frac{\pi}{2g_0} \int_0^t a_x^2(t) dt \quad (1)$$

- $I_{x-x}$ : Arias intensity in x direction  
 $a_x(t)$ : Acceleration time history in x direction  
 $t$ : Total duration of ground motion

- b. The value of the Arias intensity formula is equal to the energy of accelerogram. Since the energy

naturally is scalar, the total Arias intensity is:

$$I_h = I_{x-x} + I_{y-y} \quad (2)$$

c. Some researchers (Dobry, et al [6] and Wilson, et al [7]) believe that Arias intensity is related to the larger component of horizontal acceleration and not their sum.

d. Arias [8] defined an instrumental intensity measure integrally over the duration of the ground motion of the square of the acceleration, which has been subsequently used by several researchers to evaluate the potential damage. Harp, et al [9] found that Arias intensity correlates well with distributions of earthquake-induced landslides. Kayen, et al [5] proposed an approach to assess the liquefaction potential of soil deposits during earthquake based on Arias intensity. Cabanas, et al [10] found a good correlation between local intensity (MSK) and Arias intensity.

e. One of the most important applications of Arias intensity is to evaluate the potential of liquefaction, because the field penetration tests which are essentially energy-based, can be one of the proper criteria for evaluation of liquefaction. Kayen, et al [5] dealt with the evaluation of a field method that involves the energy of recorded ground shaking in seismographs. They also describe an approach to relate Arias intensity in the depth of soil to field-based measurements of liquefaction resistance.

f. Before using Arias intensity in evaluating the potential of liquefaction an approach developed by Seed, et al [11] that was according to field penetration and cyclic stress, was mainly used. In that approach, peak ground acceleration (PGA) is used to evaluate initial liquefaction of soil. By comparison of these two approaches, the advantages of Arias intensity over PGA can be found.

These advantages are:

- Arias intensity is derived from integration acceleration records of both horizontal components of motion, whereas PGA uses a single, arbitrarily selected value (Kayen, et al [5]).
- Arias intensity incorporates the intensity of motions over the full range of recorded frequency, whereas PGA is often associated with high-frequency motion (Kayen, et al [5]).

- The breakdown of soil structure that result to liquefaction is fundamentally more dependent on input energy than on a single level of acceleration (Liang, et al [12]).

### 3. SEISMOTECTONIC STRUCTURE OF TEHRAN

Tehran's extent is the Northeast depression of central Iran. In this region, Alborz mountains heights are forced to the Tehran plain. Being located in the North of Iranian central desert and under the Southern margin of central Alborz, the plain of Tehran has a wide variety of ground patterns. Some factors that were effective in the evolution of Tehran morphology and its surrounding mountains are [13,14]:

- Geologic factors (tectonic, rock structure, sedimentology)
- Climate factors (rainfall, temperature, plants growth, overland flow and over land soil)

Developing trend of relieves of Tehran plain during the fourth geological era and reviewing the history of the relieves formation since Pliocene (around 5 million years ago) up to now shows that periodic sedimentation and strong erosion basically have important role in the geomorphologic evolution of Tehran's extent [13,14]. Tehran plain has a Southern slope and has been divided into the following different districts by mountains and eastern-western depressions:

- High Alborz
- Alborz Border Folds
- Pediment Zone
- North Central Iranian Depression (Tehran plain)

The explanation of above-mentioned cases is beyond the scope of this paper.

As indicated previously, Tehran's extent located in the Southern district of central Alborz, obeys the seismicity regime of this region. The amount of riskability of the region with respect to probable occurrence of an earthquake depends on the performance and the activity method of faults around the city of Tehran. For Tehran's case, the faults of Fasham-Mosha, North of Tehran, Kahrizak, North

and South of Rey and some other faults existing in Tehran are the most susceptible faults which cause ground shaking. Table 1 explains the properties of the most important faults of Tehran and its vicinity.

In this paper, 24 faults were used for hazard analysis with a radius of 200 km around Tehran.

Those faults which fully or partially located in this circle were considered in our analysis.

In Table 1,  $M_{max}$  is and obtained from the fault rupture length relationship of Nowroozi [16]. Active faults of Tehran and its vicinity are illustrated in Figure 2.

**TABLE 1. Main Active Fault of Tehran and its Vicinity (Ghodrati Amiri, et al [4]).**

No	Fault	Type	Length (Km)	$M_{max}$ (Nowroozi, 1976)
1	Mosha	Thrust-Inverse	200	7.5
2	North Tehran	Thrust-Inverse	75	6.9
3	Niavaran	Thrust-Inverse	13	6
4	North Rey	Thrust-Inverse	17	6.1
5	South Rey	Thrust-Inverse	18.5	6.2
6	Kahrizak	Thrust-Inverse	40	6.6
7	Garmsar	Thrust-Inverse	70	6.9
8	Pishva	Thrust-Inverse	34	6.5

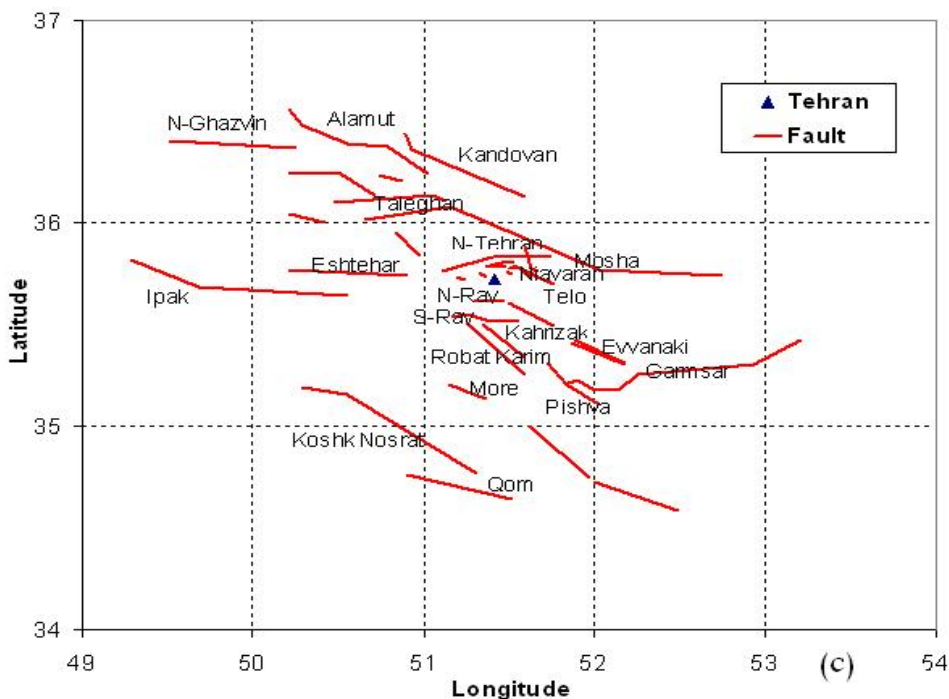


**Figure 2.** Active faults of tehran and its vicinity (Berberian, et al [15]).

#### 4. EARTHQUAKE CATALOGUE

Earthquake catalogue helps us to obtain comprehensive information about ground shaking happened in Tehran and its vicinity. The method of selecting the earthquake like previous section is to draw a circle with the radius of 200 km around the center of Tehran and to choose all earthquakes that their  $M_S$  are greater than 4 and are located inside the circle. Earthquake catalogue includes information like occurrence time, geographical latitude and longitude of the location of earthquake occurrence, type of magnitude, the value of magnitude, focal depth and distance between the location of earthquake occurrence and the center of Tehran (Ghodrati Amiri, et al [17]).

Different sources have been used for collection of earthquakes information. Some of them are:

- International Seismological Center (ISC)
- National Earthquake Information Center (NEIC)

Also the results of investigation by Ambraseys, et al [2] which is about historical earthquake (before 1900) and Moïnfar, et al [18] including collection of historical and instrumental earthquakes were used.

The catalogue used to determine the seismicity parameters, is the filtered of above catalogue. Filtering process has been done by software (Gardner, et al [19]) and includes the elimination of aftershocks and foreshocks. There are 3 types of magnitude are available in the earthquake catalogue such as follows:

- Richter local magnitude scale ( $M_L$ )
- Surface-wave magnitude scale ( $M_S$ )
- Body wave magnitude scale ( $m_b$ )

It should be noted that all magnitudes have been converted to  $M_S$ .

**4.1. Focal Depth of Earthquakes** There is a column in the catalogue (in the appendix of paper) called FD, which shows the focal depth of earthquakes. In some earthquake cases the value of this column has been left blank indicating the lack of information regarding the earthquakes. Also, considering that most earthquakes in Iran are shallow, some of these values seem to be unreasonable. Determining exact value of focal

depth needs an exact network that unfortunately doesn't exist in Iran. In this paper, the value of focal depth ( $h$ ) is considered 10 km whereas it isn't specified by developers of attenuation relationships. It should be kept in mind that the variation of focal depth has minor effect on results.

**4.2. The Magnitude of Earthquake** The magnitude usually used in seismic hazard analysis is  $M_S$ . Also  $m_b$  will be used in special cases. In this paper, IRCOLD relationship [20] is used to convert  $m_b$  in to  $M_S$ . This relationship is expressed as follows:

$$M_S = 1.2m_b - 1.29 \quad (3)$$

The correlation coefficient of this relationship is

$$R^2 = 0.87$$

#### 5. DETERMINATION OF SEISMICITY PARAMETERS

Seismic hazard analysis needs determination of seismicity parameters and potential of earthquakes occurrence in the future. Parameters used in this paper are:

- Maximum expected magnitude ( $M_{max}$ )
- $b$  value of Gutenberg-Richter relationship [21]
- Activity rate ( $\lambda$ )

Two approaches are used to determine these parameters:

- Kijko method [22]
- Tavakoli's approach [23]

**5.1. Kijko Method [22]** The first method to determine parameters is to use Kijko method [22]. This method provides numerous capabilities, particularly for the data of seismic events that are not uniform (Ghodrati Amiri, et al [24]). Therefore, it can be employed for processing the seismic data of Iran. For this purpose, three input files should be prepared. The first file contains earthquakes before 1900 (Case#1) with uncertainty of 0.3-0.5 (0.5 is considered only for earthquake of the 4<sup>th</sup> BC and 0.3 is need for other earthquakes). The second

file contains earthquakes between 1900 and 1963 (Case#2). The uncertainty of these earthquakes is 0.2. The third file contains earthquakes between 1964 and 2007 (Case#3). The uncertainty of these earthquakes is 0.1. Table 2 shows the outputs of Kijko method. It should be noted that  $\beta = b \cdot \ln 10$  [22].

One of the main advantages of this method, which accounts for its superiority over the other approaches, is its use of the appropriate statistical methods, which are up-to-date and correspond with the employed distribution functions such as the maximum likelihood estimation method (Ghodrati Amiri, et al [24]). While using the Kijko method [22], seismicity properties in the range of 200 km around Tehran are considered equal and homogeneity.

Another important point is that using historical earthquakes (to increase time span of the catalogue and increasing the obtained authenticity) and instrumental earthquakes (for their accuracy and completeness) will improve the validity of results (Ghodrati Amiri, et al [4]).

In Figure 3 the annual rate of occurrence,  $\lambda$ , for earthquakes with magnitude greater than 4 is presented.

**5.2. Tavakoli's Approach [23]** In a paper by Tavakoli [23], Iran is divided into 20 seismotectonic provinces where Tehran is in the 15<sup>th</sup> province (Figure 4). In that paper, a method is introduced for determining coefficients of Gutenberg-Richter relationship [21]. Gutenberg and Richter presented this logarithmic relationship for seismic hazard analysis.

$$\log(n(m)) = a - b \times m \quad (4)$$

Where  $n(m)$  is activity rate ( $\lambda$ ),  $m$  is the earthquake magnitude, (a) and (b) are coefficients of equation. In the 15<sup>th</sup> province of Tavakoli [23] the coefficients of a and b are 1.908 and 0.52.

Table 3 shows another result of Tavakoli's approach [23].

## 6. SEISMIC HAZARD ASSESSMENT

In this section the values of Arias intensity for four hazard level are obtained by using the SEISRISKIII software (Bender, et al [25]). These hazard levels are derived from the instruction for seismic rehabilitation of existing building [26] and their values are: 2, 10, 20, and 50 percent hazard in 50 year. The corresponding return periods with these time periods are: 72, 224, 475, 2475 years.

The network which hazard analysis has been done for it, covers of Tehran, is a square-shaped and at 30×30 km. It is divided into squares with dimensions of 1×1 km and for each site of this network, probabilistic Arias Intensity has been obtained. Geotechnical map of this network was available [13,14].

**6.1. Attenuation Relationships** One of the most important parts of seismic hazard assessment is attenuation relationship. Attenuation relationship describes decrease in the ground motion as a function

TABLE 2. Seismicity Parameters in Different Cases for Tehran.

Catalogue	Parameter	Value	Data Contribution to the Parameters (%)		
			Case # 1	Case # 2	Case # 3
Instrumental Earthquake Data	Beta	1.45		33.3	33.6
	Lambda (for $M_S=4$ )	0.83		19.7	80.3
Historical Earthquake Data	Beta	2.4	100		
	Lambda (for $M_S=4$ )	0.22	100		
Historical and Instrumental Data	Beta	1.63	34.4	32.7	33
	Lambda (for $M_S=4$ )	0.85	19.5	15.9	64.6

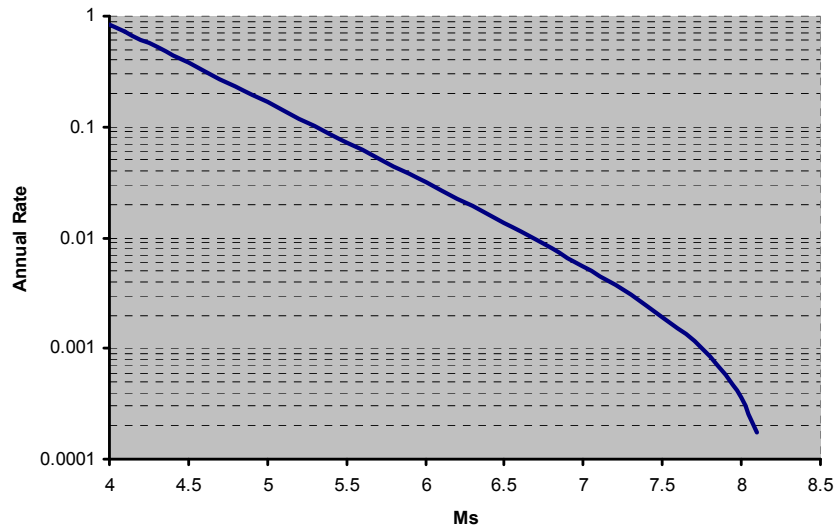


Figure 3. Annual rates estimated by the Kijko method [22] for Tehran and its vicinity.

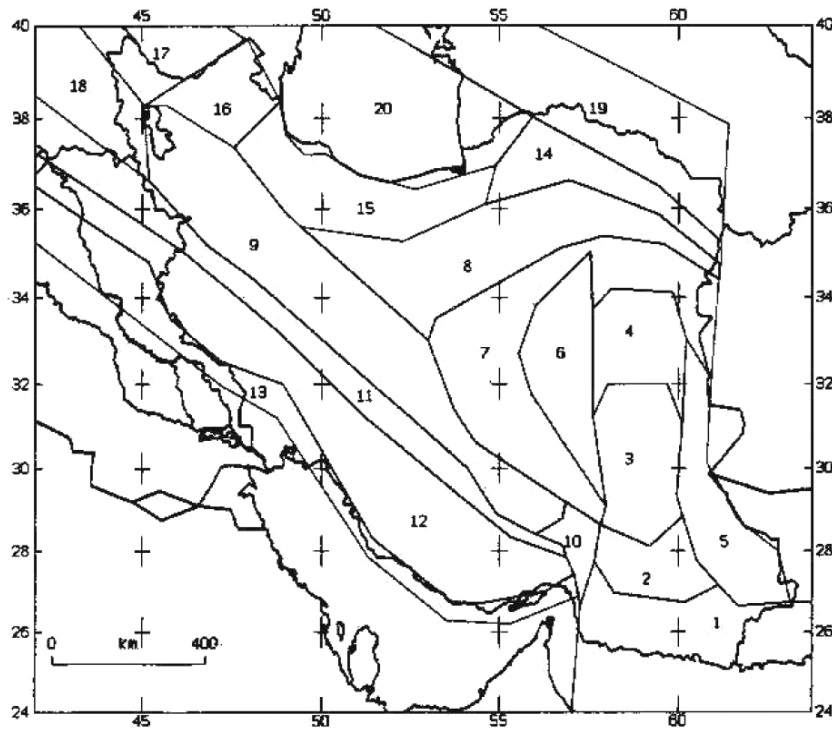


Figure 4. Seismotectonic provinces of iran (Tavakoli [23]).

TABLE 3. Seismicity Parameters for Seismotectonic Province of Tehran (Tavakoli [23]).

Province No.	Span of Time	Beta	$M_{max}$	Lambda
15	1927-1995	$1.41 \pm 0.11$	$7.9 \pm 0.3$	0.37

of distance and magnitude. Many factors affect the attenuation relationships which are: the geology effects of the site, source specifications, magnitude, fault mechanism, reflection and refraction, etc (Ghodrati Amiri, et al [17]). The general form of attenuation relationship is:

$$\log(y) = a + F_1(M) + F_2(R) + F_3(S) + \varepsilon \quad (5)$$

Where

- y: Parameter of ground motion (for example Arias intensity)  
a: Constant of equation  
 $F_1(M)$ : Is a function in terms of magnitude which is proportional to y.  
 $F_2(R)$ : Is a function in terms of distance which is inverse proportional to y.  
 $F_3(S)$ : Is a function that models the site condition, fault mechanism, thickness of sediment, etc.  
 $\varepsilon$ : Is a random error with mean value of zero and standard deviation of  $\sigma$  representing uncertainty in Y

In this paper, four attenuation relationships were used that are explained as follows.

**6.1.1. MahdaviFar, et al [27]** This relationship derived from 22 strong motion records generated by 19 earthquakes in Alborz and central Iran. The relationship is expressed as follows:

$$\log(I_a) = -3.880 + 0.810M - \log(R) - 0.002R \pm 0.46P \quad (6)$$

Where  $I_a$  is Arias intensity in m/s., M is moment magnitude, R is source to site distance in km, and p is 0 for 50 percentile values and 1 for 84 percentiles. It should be stated some points about above relationship:

$$I_a = \text{Max}(I_{x-x}, I_{y-y}) \quad (7)$$

$$R = \sqrt{r^2 + h^2} \quad (8)$$

Where r is defined as the closest distance between accelerometer stations and the fault rupture plane and h is focal depth (h =10 km). The developers of this relationship have considered the effect of type of soil in determining coefficients of equation.

**6.1.2. Travasarou, et al [28]** The strong motion dataset in this relationship includes 1208 records from 75 earthquakes having magnitudes ranging from 4.7 to 7.6. The dataset is based on the worldwide data from shallow crustal earthquake.

The general form of this relationship is:

$$\begin{aligned} \ln(I_a) = & 2.8 - 1.981 \times (M - 6) + 20.72 \times \ln(M/6) - \\ & 1.703 \times \ln(\sqrt{R^2 + h^2}) + (0.454 + 0.101 \times (M - 6)) \times \\ & S_C + (0.479 + 0.334 \times (M - 6)) \times \\ & S_D - 0.166 \times F_N + 0.512 \times F_R \end{aligned} \quad (9)$$

Where  $I_a$  is the Arias intensity in m/s., M is the moment magnitude, R is the closest distance to the rupture plane in km.

- $S_C, S_D$ : indicator variables for the soil types  
 $S_C = 0, S_D = 0$ , Site category B  
 $S_C = 1, S_D = 0$ , Site category C  
 $S_C = 0, S_D = 1$ , Site category D
- $F_N, F_R$ : Indicator variables for the fault types. Since the most faults in the city of Tehran are thrust and reverse type, therefore:  
 $F_N = 0, F_R = 1$
- The error term of equation is normally distributed with mean zero and standard deviation  $\sigma_{tot}$ .

$$\sigma_{tot}(M, I_a) = \sqrt{\sigma(I_a, \text{site})^2 + \tau^2(M)} \quad (10)$$

$$\tau(M) = 0.611 - 0.047 \times (M - 4.7) \quad 4.7 \leq M \leq 7.6 \quad (11)$$

$$\sigma(I_a, \text{site}) = \begin{cases} \sigma_1 & I_a \leq 0.013 \text{ m/s} \\ \sigma_1 - 0.106 \times (\ln(I_a) - \ln(0.0132)) & 0.013 < I_a < 0.125 \text{ m/s} \\ \sigma_2 & I_a \geq 0.125 \text{ m/s} \end{cases} \quad (12)$$

Where

- $\sigma_1 = 1.18, \sigma_2 = 0.94$  for site B
- $\sigma_1 = 1.17, \sigma_2 = 0.93$  for site C
- $\sigma_1 = 0.96, \sigma_2 = 0.73$  for site D

Since in the SEISRISK III [25] input file, it should be inserted a single value for “ $\sigma$ ” for each attenuation relationship.



Site B:  $760 < V_s < 1500$  m/s, Site C:  $360 < V_s < 760$  m/s, Site D:  $180 < V_s < 360$  m/s

- The earthquake records of Tabas, Iran [1978] are among the 1208 records used.
- $h = 8.78$

$$I_a = (I_{x-x} + I_{y-y})/2 \quad (13)$$

**6.1.3. Kayen, et al [5]** Records of 66 earthquakes happened in California are used in developing this relationship. Coefficients of this relationship are obtained for three types of sites namely rock, alluvium and soft.

Rock sites:

$$\log(I_h) = M - 4.0 - 2\log(r^*) + 0.63P \quad (14)$$

Alluvium sites:

$$\log(I_h) = M - 3.8 - 2\log(r^*) + 0.61P \quad (15)$$

Soft sites:

$$\log(I_h) = M - 3.4 - 2\log(r^*) \quad (16)$$

$$r^* = \sqrt{r^2 + \Delta^2} \quad (17)$$

$$I_h = I_{x-x} + I_{y-y} \quad (18)$$

- $\Delta = 10$  km
- $M$  = moment magnitude
- The term of standard deviation is not seen in the relationship associated with soft soil because of the lack of sufficient information to determine it.

**6.1.4. Tselentis, et al [29]** The strong motion records used in this relation were selected from Greek accelerograms provided by the European strong motion data base.

The coefficients of this relationship are obtained for 3 types of sites namely rock, stiff soil and soft soil.

Rock:

$$\log(I_a) = 0.74 \times M - 1.56 \times \log(\sqrt{R^2 + h^2}) - 3.49 + \epsilon_{\text{Rock}} \quad (19)$$

Stiff Soil:

$$\log(I_a) = M - 1.57 \times \log(\sqrt{R^2 + h^2}) - 4.8 + \epsilon_{\text{StiffSoil}} \quad (20)$$

Soft Soil:

$$\log(I_a) = 1.18 \times M - 1.811 \times \log(\sqrt{R^2 + h^2}) - 5.23 + \epsilon_{\text{SoftSoil}} \quad (21)$$

- Rock:  $V_s > 800$  m/s, Stiff Soil:  $360 < V_s < 665$  m/s and Soft Soil:  $200 < V_s < 360$  m/s
- $h = 7$  km
- $M$  = moment magnitude
- $\epsilon_{\text{rock}} = 0.679$ ,  $\epsilon_{\text{stiff}} = 0.52$ ,  $\epsilon_{\text{soft}} = 0.305$

$$I_h = I_{x-x} + I_{y-y} \quad (22)$$

About above relationships:

- Only limited attenuation relationships have been presented for Arias intensity all over the world. Hence, we didn't encounter different options for selection of above-mentioned relationships.
- Some relationships weren't compatible with condition of our considered region. For example, there are some relationships that " $M_L$ " is used in their formula or they are not classified according to the type of soil. Furthermore, the range of the magnitude that used in some relationships is very limited whereas in all relationships that used in this paper, it is impossible to utilize magnitudes between 4.5 and 7.5.

## 6.2. Relationships Between Maximum Expected Magnitude and Fault Rupture Length

The relationship between the maximum expected magnitude and fault rupture length depends on the understanding of the seismotectonic and geotectonic behavior of the concerned area (Ghodrati Amiri, et al [4]).

The general form of relationship between maximum expected magnitude and fault rupture length is as follows:

$$\log(L) = a + b \times M \quad (23)$$

Where  $L$  is the rupture length,  $M$  is the maximum

expected magnitude and (a) and (b) are constant coefficients. The rupture length is a percentage of the length where this percentage lies between 30 and 50 (Tavakoli [30]).

In this paper, two fault rupture length relationships are used. The first relationship comes from Nowroozi's work [16] that belongs to Iran and the second relationship comes from Wells, et al's work [31] that is obtained based on the collection of historical earthquakes around the world.

**6.2.1. Nowroozi [16]** This relationship is obtained based on the studies on 10 strong earthquake and the faults caused them. Among these faults, it can be pointed to Zagros fault, North Alborz fault and North Tabriz fault. The relationship suggested by Nowroozi [16] is expressed as follows:

$$\log(L) = -0.126 + 0.675 \times M_S \quad (24)$$

$M_s$  is the surface magnitude and  $L$  is the rupture length in meter. The correlation coefficient of the above relationship is  $R^2 = 0.87$  [16].

**6.2.2. Wells, et al [31]** The information of 244 historical earthquakes is used to develop this relationship. Among the most important characteristics, the two followings could be pointed out:

- Hypocentral depth < 40 km
- $M_w > 4.5$

$$\log(L) = -3.22 + 0.69 \times M_W \quad (25)$$

Where  $M$  is the moment magnitude and  $L$  is the surface rupture length in kilometer. It should be noted that 12 earthquakes in Iran are seen among 244 earthquakes established in the paper of Wells, et al [31].

**6.3. Logic Tree** In the previous sections, attenuation relationships, fault rupture length relationships and methods of determining seismicity

Parameters were discussed. In order to combine these relationships and to perform probabilistic seismic hazard analysis (PSHA), logic tree should be used. Logic tree is a popular tool used to compensate for the uncertainty in PSHA (Ghodrati Amiri, et al [4]).

The reason for using different relationship in this paper is the non-existence of appropriate

accelerogram network in Iran that leads to the lack of data and the lack of accuracy for existing data. Figure 5 shows the logic tree considering the uncertainty of attenuation relationships, seismicity parameters and fault rupture length relationship.

#### 6.4. Probabilistic Seismic Hazard Analysis

Seismic hazard is the expected occurrence of a future adverse earthquake that has implication of future uncertainty; therefore, the theory of probability is used to predict it [32]. The probabilistic approach, used in this study, takes into consideration the uncertainties in the level of earthquake magnitude, its hypo central location, its recurrence relationship and its attenuation relationship [33].

The steps for seismic hazard assessment can be summarized as follows:

- (1) Modeling of seismic sources,
- (2) Evaluation of recurrence relationship (i.e. frequency-magnitude relation),
- (3) Evaluation of attenuation relationships for peak ground acceleration,
- (4) Estimation of activity rate for probable earthquakes,
- (5) Evaluation of basic parameters such as maximum magnitude,
- (6) Evaluation of local site effects such as soil types, geotechnical characteristics of sediments, topographic effects, etc. [34-38].

Steps 1 through 5 represent seismic hazard assessment for an ideal "bedrock" conditions while the inclusion of step 6 represents seismic hazard assessment for a specific site.

As stated before, in this paper, SEISRISK III software [25] was used for PSHA. There are more advanced SHA programs than SEISRISK III software [25] which can perform Seismic hazard analysis more accurately. However it was preferred to use this software due to the lack of data and accuracy. Seismic hazard maps in terms of Arias intensity in Tehran and its vicinity using Logic Tree for 72, 225, 475 and 2475 years return period are plotted as iso-intensity contours in desired periods in Figures 6-9.

## 7. CONCLUSION

In this paper, the seismic hazard analysis of city of

Fault Rupture Length Relationships

Seismicity Parameters

Attenuation Relationships

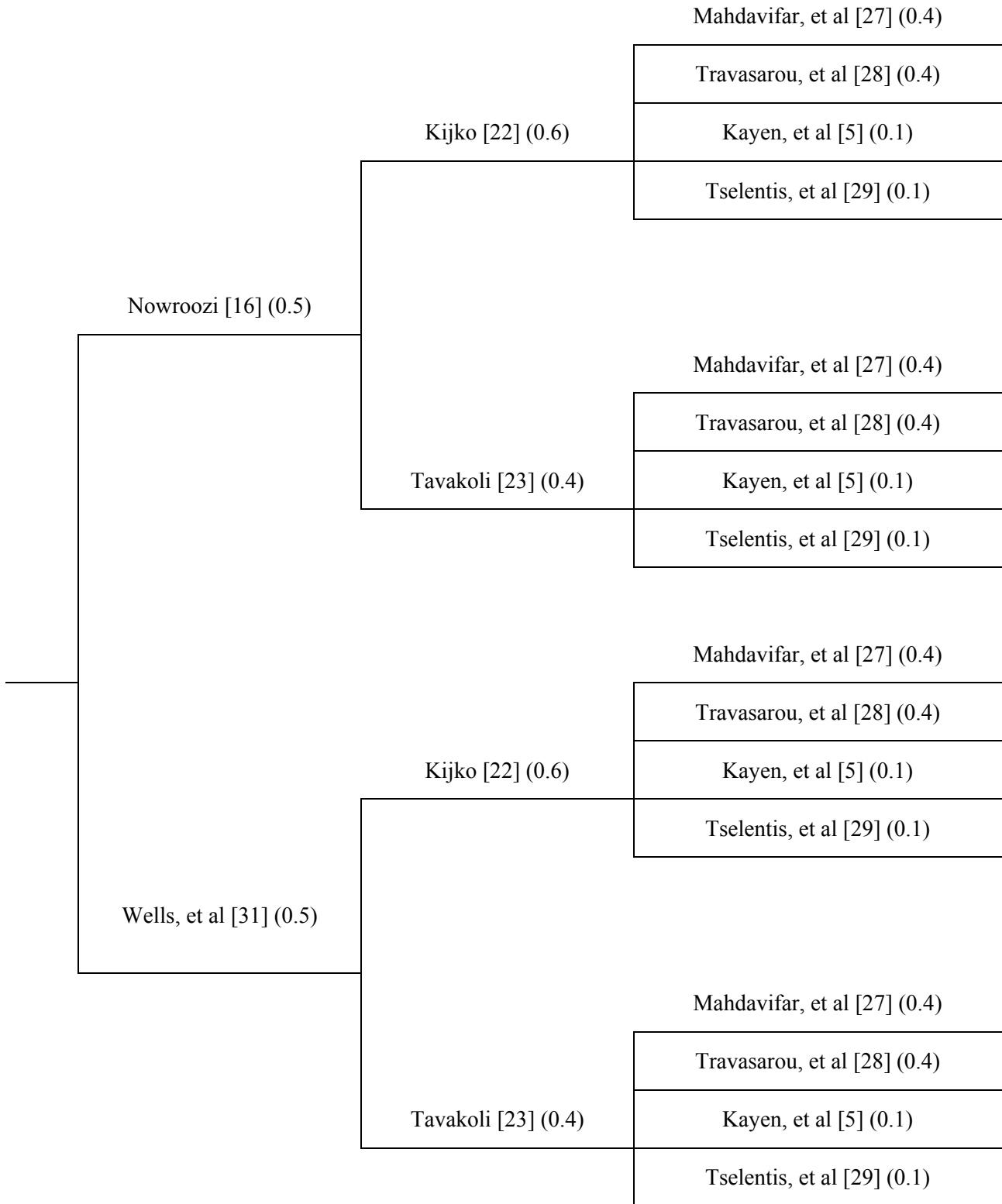
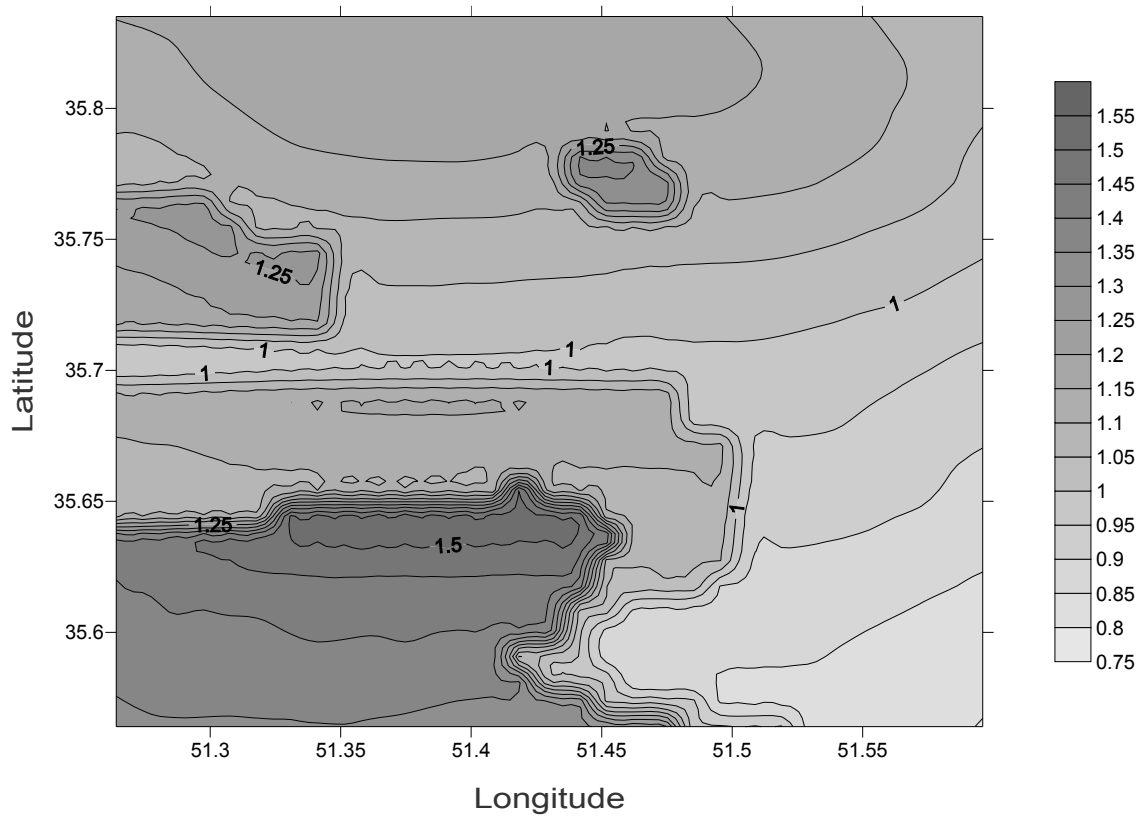
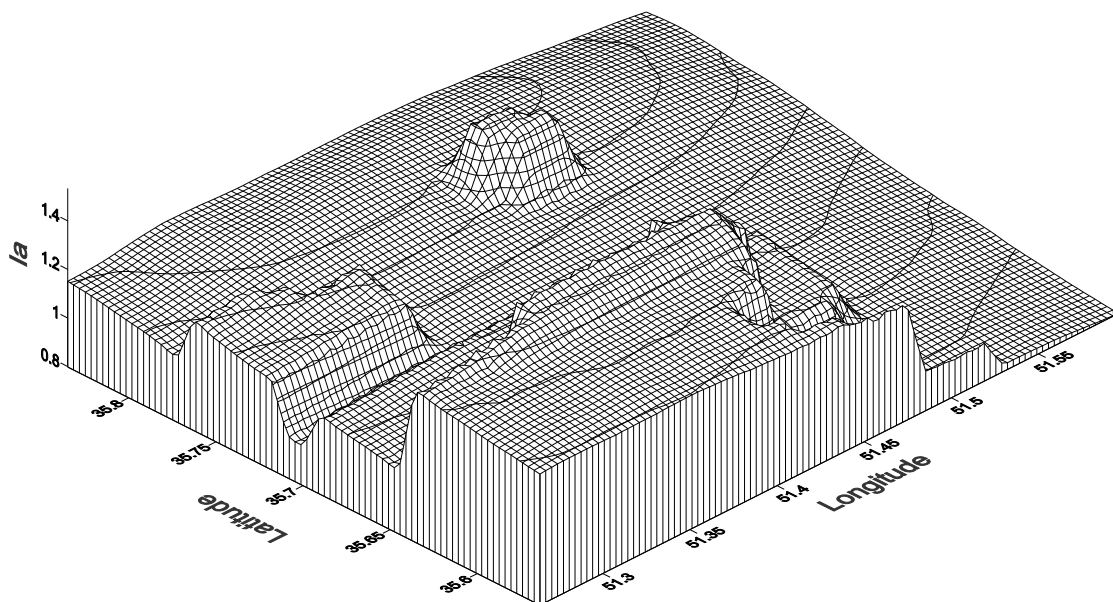


Figure 5. Applied logic tree.

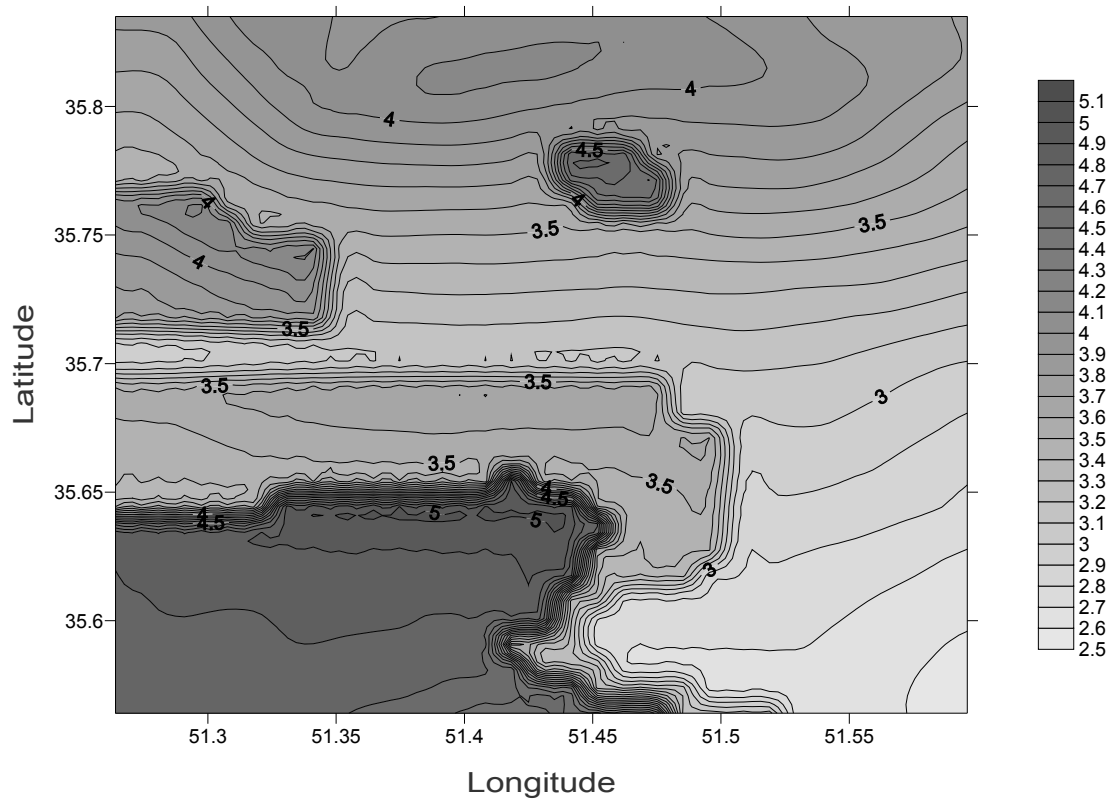


(a)

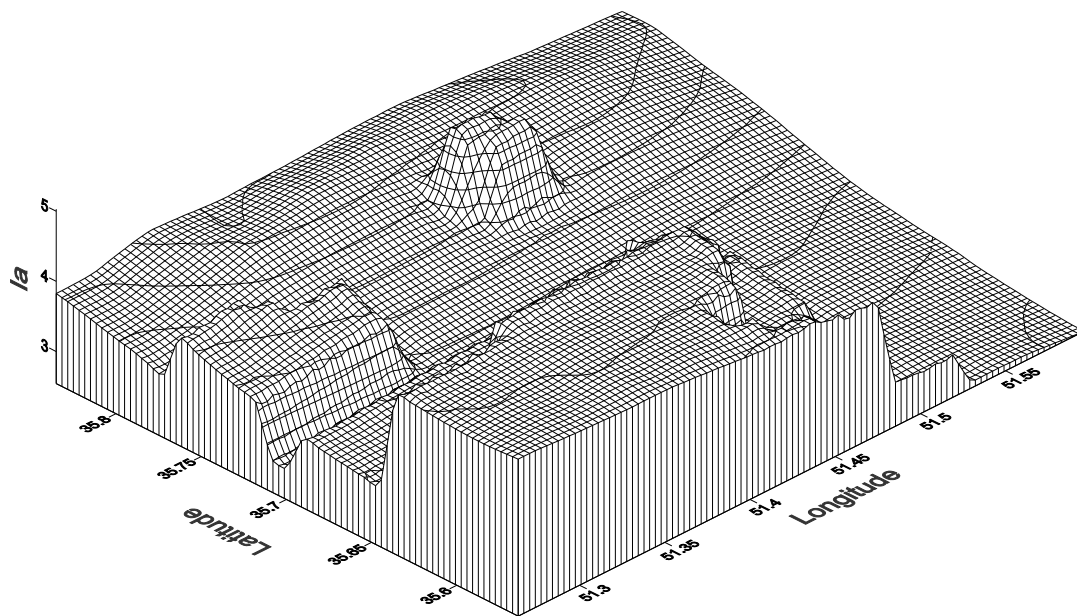


(b)

**Figure 6.** Seismic hazard maps in terms of arias intensity in tehran and its vicinity using logic tree for 72 years return period (a) two-dimensional zoning map showing Arias intensity (b) three-dimensional zoning map showing arias intensity.

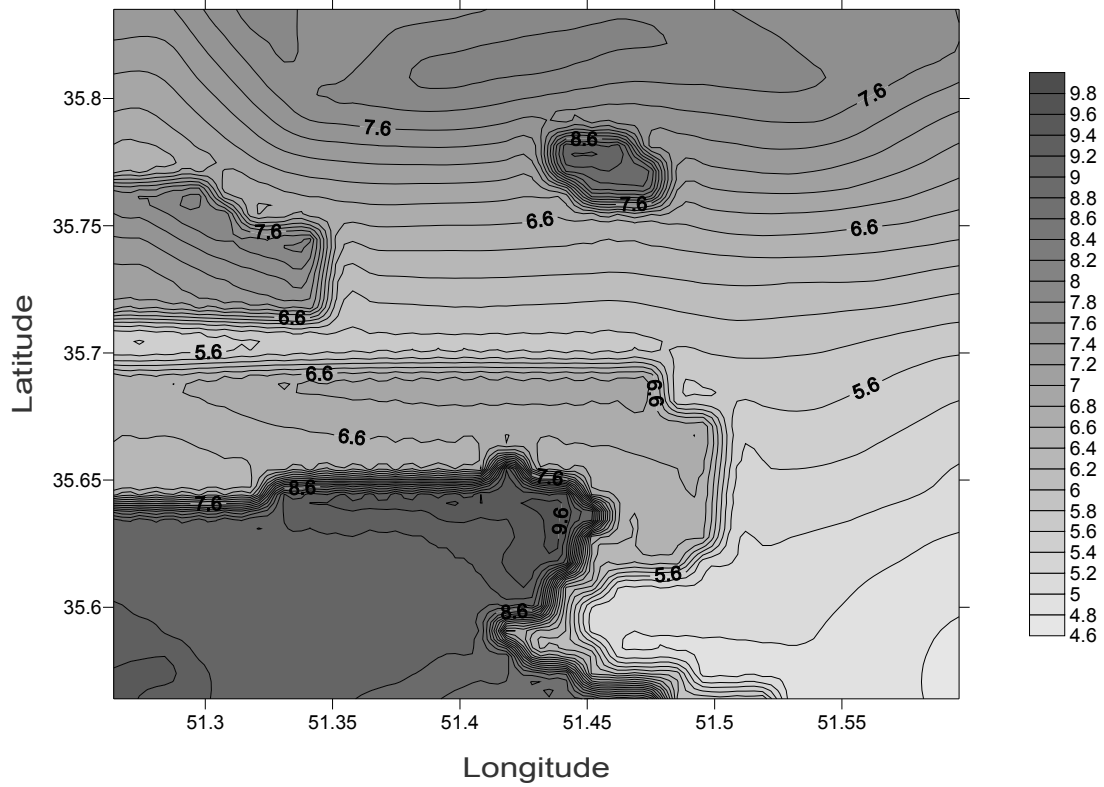


(a)

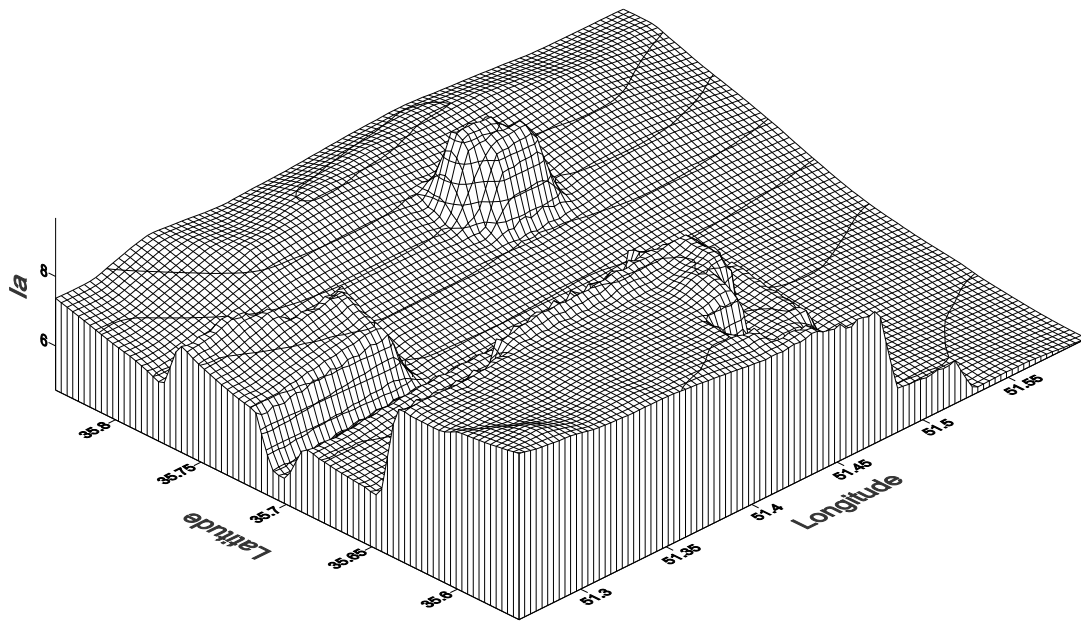


(b)

**Figure 7.** Seismic hazard maps in terms of arias intensity in tehran and its vicinity using logic tree for 224 years return period (a) two-dimensional zoning map showing arias intensity (b) three-dimensional zoning map showing arias intensity.

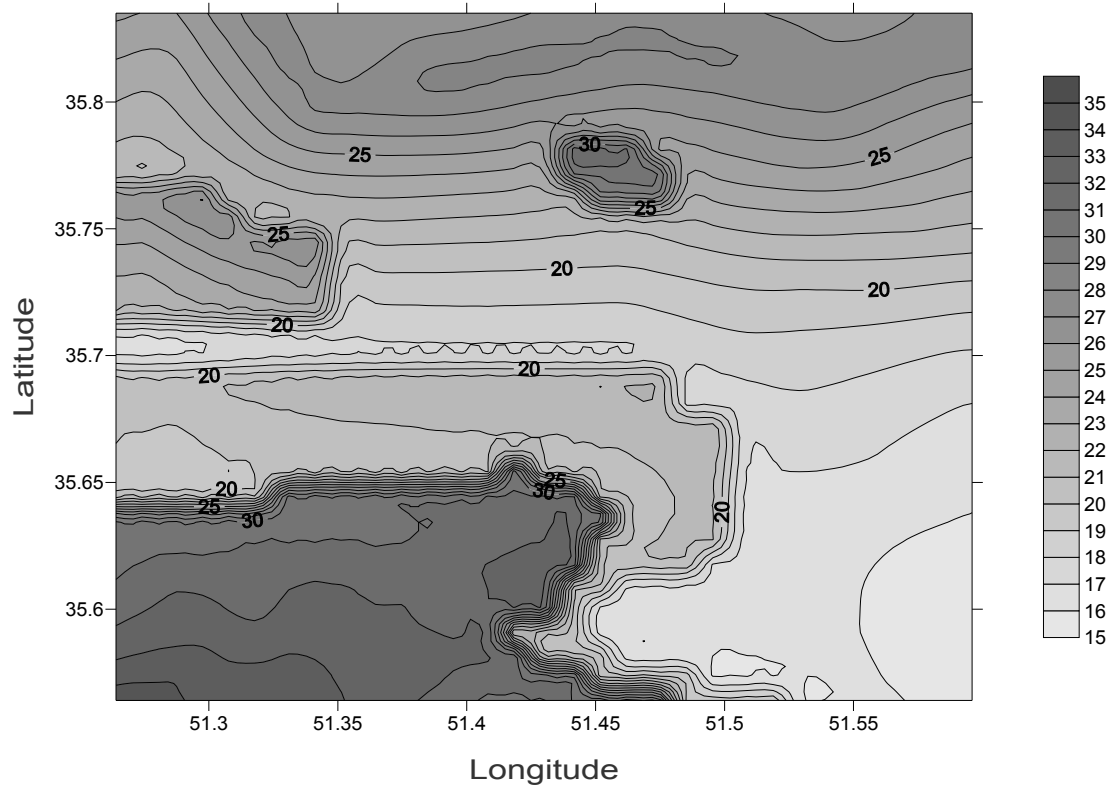


(a)

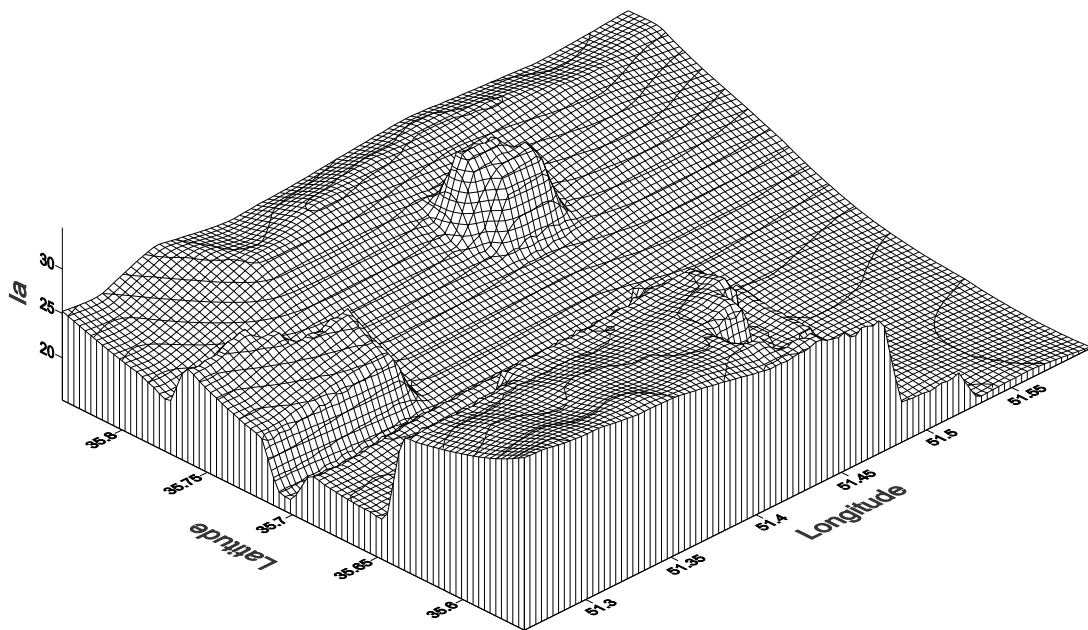


(b)

**Figure 8.** Seismic hazard maps in terms of arias intensity in tehran and its vicinity using logic tree for 475 years return period (a) two-dimensional zoning map showing arias intensity (b) three-dimensional zoning map showing arias intensity.



(a)



(b)

**Figure 9.** Seismic hazard maps in terms of arias intensity in tehran and its vicinity using logic tree for 2475 years return period (a) two-dimensional zoning map showing arias intensity (b) three-dimensional zoning map showing arias intensity.

Tehran is performed by using Arias intensity parameter. Important results of this analysis are expressed as follows:

1. Developing a full and up-to-date catalogue (by using the information of historical and instrumental earthquakes)
2. Determining seismicity parameters of city of Tehran.
3. Drawing Iso-intensity maps according to the type of soil for city of Tehran and based on the different attenuation relationships, fault rupture length relationships and the methods of determining seismicity parameters.

4. By paying attention to the curves, it can be noticed that whenever soil type changes from rocky to stiff, there is an increase in the Arias in that region.
5. In some parts of Tehran, due to approaching to the faults and also being situated over small or large faults of the region, there will be higher Arias than other points.

As stated previously, liquefaction and landslides have close relationship with Arias Intensity. The results of this paper can be helpful to determine the points of liquefaction of Tehran and also those regions that are susceptible to landslide.

## 8. APPENDIX

### 8.1. Earthquake Catalogue.

No	Date			Earthquake Time (h:m:s)	Epicenter		FD (km)	Magnitude			References	Distance (km)
	Year	Month	Day		Lat	Long		M <sub>S</sub>	m <sub>b</sub>	M <sub>L</sub>		
1	4 <sup>th</sup> BC				35.5	51.8		7.6			AMB	38
2	743				35.3	52.2		7.2			AMB	80
3	855				35.6	51.5		7.1			AMB	11
4	864	1			35.7	51		5.3			AMB	35
5	958	2	23		36	51.1		7.7			AMB	46
6	1119	12	10	1800	35.7	49.9		6.5			AMB	129
7	1127				36.3	53.6		6.8			AMB	200
8	1177	5			35.7	50.7		7.2			AMB	61
9	1301				36.2	53.4		6.5			NEIC	188
10	1485	8	15	1800	36.7	50.5		7.2			AMB	140
11	1495				34.5	50		5.9			AMB	179
12	1608	4	20	1200	36.4	50.5		7.6			AMB	113
13	1665				35.7	52.1		6.5			AMB	59.4
14	1678	2	3	600	37.2	50		6.5			AMB	211
15	1687				36.3	52.6		6.5			AMB	125
16	1755	6	7	1200	34	51.4		5.9			AMB	188
17	1778	12	15	2400	34	51.3		6.2			AMB	189
18	1808	12	16	1800	36.4	50.3		5.9			AMB	126
19	1809			1200	36.3	52.5		6.5			AMB	118
20	1825				36.1	52.6		6.7			AMB	113
21	1830	4	6	1200	35.7	52.3		7.1			AMB	76
22	1868	8	1	2000	34.9	52.5		6.4			AMB	128
23	1901	5	20	122900	36.39	50.48		5.4			AMB	114
24	1927	7	22	35510	34.9	52.9		6.3	6.3		AMB	223
25	1930	10	2	153312	35.76	51.99	33	5.2			AMB	49



26	1932	5	20	191611	36.5	53.5		5.5	5.6		USGS	202
27	1935	4	11	2315	36.5	53.3	14	6.3			NEIC	192
28	1940	9	25	193120	36.2	52.2		4.8	5		CCP	90.5
29	1945	5	11	201728	35.18	52.4	33	4.4	4.7		BER,M	101
30	1948	6	30	193150	36.66	49.48	114	4		5	NOW	200
31	1951	11	13	140146	35.7	53.2		4.1	4.5		CCP	154
32	1954	9	2	224700	35.3	52		4.1	4.5		CCP	66
33	1956	4	12	223449	37.33	50.26	30	5		5.5	NOW	212
34	1957	5	6	141950	37.2	51.8	12	4.5	4.8		NOW	207
35	1957	7	2	4222	36.07	52.47		7.2	7		AMB	177
36	1958	1	16	22500	36.5	53		4.3	4.6		PT	166
37	1958	11	2	91428	36.7	51.5		4.1	4.5		BCIS	
38	1960	6	23	132308	34.5	50.5		4	4.4		BAN	160
39	1961	2	11	193600	37	50		4.1	4.5		PT	193
40	1962	9	1	192050	35.71	49.81	21	7.1	6.9		AMB	114
41	1964	2	8	62823	37.07	50.99	11	4.3	4.6		NOW	
42	1966	10	3	170508	35.8	53.44	14	4.6	4.9		ISC	
43	1966	11	8	31414	36.1	50.8	38	4.8	5		USGS	68
44	1967	2	16	115532	35.74	51.88	16	4	4.4		CGS	42
45	1967	8	25	122650	35.58	49.33	55	4.4	4.7		ISC	
46	1968	4	26	25822	35.1	50.2	21	5.1	5.3		USCGS	
47	1968	5	19	164950	36.61	53.35	22	4.3	4.6		ISC	198
48	1968	12	12	185447	35.8	53.49	27	4.6	4.9		ISC	179
49	1970	6	27	75758	35.2	50.7	14	4.6	4.9		USGS	81
50	1971	4	30	90616	34.6	50.3	42	4.4	4.7		USCGS	
51	1971	8	9	25435	36.27	52.81	12	5	5.2		ISC	138
52	1972	1	30	90617	34.68	50.33	38	4.4	4.7		ISC	145
53	1972	2	23	231337	36.2	53.5	73	4	4.4		ISC	189
54	1972	8	8	4455	36.3	52.6	47	4.4	4.7		USCGS	
55	1973	9	17	40602	36.5	51.19	40	4.4	4.7		ISC	95
56	1974	11	5	200221	36.29	53.01	40	4.3	4.6		ISC	154
57	1975	4	11	142646	35.65	50.35	59	4.4	4.7		ISC	91
58	1975	11	6	40931	35.9	53	3	4.4	4.7		NEIS	139
59	1977	4	6	133700	34	50		6.4		6.2	HFS1	224
60	1977	5	25	110147	34.91	52.06	39	5.1	5.3		ISC	102
61	1978	5	26	134291	37	50		6.3	6.3		HFS1	193
62	1978	11	3	185259	37	51		4.8	5		HFS	154
63	1978	11	4	152141	34	51		6.7	6.6		HFS	192
64	1979	3	18	51951	36.48	52.64	33	4.1	4.5		USCGS	
65	1979	3	25	23226	34.9	52.46	48	4.3	4.6		ISC	125
66	1980	7	22	51710	37.19	50.2	62	5.2	5.4		USCGS	
67	1980	12	19	11656	34.58	50.65	33	5.8			USCGS	
68	1981	8	4	185360	36.45	51.27		4.4	4.7		ISC	89
69	1982	2	5	233712	36.1	53.7	33	4.1	4.5		ISC	202
70	1982	7	5	155424	34.63	51.02	33	4	4.4		USCGS	
71	1982	10	25	165452	35.13	52.38	44	4.1	4.5		ISC	103
72	1983	3	26	40719	35.96	52.22	33	5.2	5.4		NEIC	80

73	1983	5	29	171540	35.24	52.17	39	4	4.4		ISC	81
74	1983	12	20	222101	36.92	50.91	26	4.5	4.8		ISC	147
75	1984	9	9	175459	35.58	49.34	33	4.3	4.6		NEIC	186
76	1985	2	11	92645	34.56	50.67	50	4.4	4.7		NEIC	142
77	1985	7	8	170236	36.27	53.71	33	4.4	4.7		ISC	209
78	1985	10	14	152831	35.52	52.7	10	4.4	4.7		ISC	112
79	1986	3	20	151809	36.01	53.68	34	4.3	4.6		ISC	199
80	1987	11	25	20938	35.7	53.07	33	4	4.4		ISC	143
81	1988	1	14	112920	36.01	50.6	33	4.3	4.6		NEIC	79
82	1988	3	1	10203	34.48	50.79	16	4.2	4.5		ISC	145
83	1988	8	22	212335	35.28	52.35	10	4.7	5		NEIC	91
84	1990	1	20	12710	35.89	53	25	5.3	5.5		ISC	139
85	1990	6	20	21001	36.99	49.35	10	7.4			ISC	232
86	1991	1	22	120422	35.57	52.4	13	4.3	4.6		USGS	
87	1991	8	23	221421	35.9	53.25	33	4.4	4.7		NEIC	160
88	1991	9	8	42035	35.32	53.31	66	4.1	4.5		USGS	
89	1992	9	22	140555	36.3	52.65	33	4.7	5		NEIS	128
90	1993	3	8	191321	36.63	51.08	33	4	4.4		NEIC	110
91	1993	6	9	173336	34.76	53.27	30	4.7	5		NEIC	197
92	1993	8	19	100428	35.09	52.09	18	4.3	4.6		NEIC	89
93	1994	11	21	185516	35.9	51.88	33	4.2	4.5		NEIC	49
94	1995	6	26	211255	36.56	51.2	33	4.2			NEIC	100
95	1996	8	25	141708	35.96	52.95	33	4	4.4		NEIC	143
96	1997	6	7	202948	36.41	50.28	33	4	4.4		NEIC	130
97	1997	8	26	4449	36.54	53.07	33	4.2	4.5		NEIC	177
98	1997	11	5	224256	34.98	51.36	33	4.2	4.5		NEIC	76
99	1998	1	9	190613	36.47	52.17	33	4.5	4.8		NEIC	112
100	1998	12	3	131333	36.05	50.88	33	4.2	4.5		NEIC	63
101	1999	3	13	43015	35.38	53.46	33	4.2	4.5		NEIC	188
102	2002	4	8	183058	36.42	52.03	46	4.5	4.8		BHRC	98
103	2002	4	19	134649	36.57	49.81	33	5	5.2		BHRC	172
104	2002	5	21	104837	36.35	51.56	33	4	4.4		BHRC	73
105	2002	10	10	121343	35.89	52.33	33	4.4	4.7		BHRC	86
106	2003	6	21	150006	35.62	52.91	33	4.2	4.5		USGS	137
107	2003	12	24	34957	35.12	50.51	10	4.4	4.7		USGS	103
108	2004	5	28	123844	36.29	51.61	17	6.3			USGS	68
109	2004	8	21	135318	35.43	49.46	10	4.2	4.5		USGS	178
110	2005	2	20	4613	36.56	52.89	30	4.3	4.6		USGS	165
111	2005	3	25	124854	35.01	50.05	14	4.4	4.7		USGS	144
112	2005	9	5	93018	34.18	52.04	10	4.5	4.8		USGS	178
113	2007	6	18	142949	34.49	50.82	10	5.3	5.5		USGS	144

**Table Notification:**

**AMB:** Ambraseys, N.N., Melville, C.P., **BCIS:** Bureau Central International de Seismologie, Strasbourg, France, **BER, M:** Berberian, Geological and Mining Survey of Iran, **BHRC:** Building and Housing Research Center, **CCP (BAN):** Atlas USSR Earthquake, **FS (BAN):** Fisher, **HFS1:** Hagfors, Sweden, **ISC:** International Seismological Center, U.K., **MOS:** Moscow, USSR **NOW:** Nowroozi, **NEIC:** National Earthquake Information Center, U.S.A., **NEIS:** National Earthquake Information Service, U.S.A., **PT:** Publication of Institute of Geophysics\_Tehran University, **USCGS:** US Coast and Geodetic Survey, U.S.A., **USGS:** United States Geological Survey.

## 9. REFERENCES

1. Tavakoli, B. and Ghafory-Ashtiany, M., "Seismic Hazard Assessment of Iran", *Annali Di Geofisica*, Vol. 42, (1999), 1013-1021.
2. Ambraseys, N.N. and Melville, C.P., "a History of Persian Earthquake", Cambridge University Press, Cambridge, Britain, (1982), 1-22.
3. Hwang, H., Lin, C.K., Yeh, Y.T., Cheng, S.N. and Chen, K.C., "Attenuation Relations of Arias Intensity Based on the Chi-Chi Taiwan Earthquake Data", *Soil Dynamic and Earthquake Engineering*, Vol. 24, (2004), 509-517.
4. Ghodrati Amiri, G., Motamed, R. and ES-Haghi, H.R., "Seismic Hazard Assessment of Metropolitan Tehran, Iran", *Journal of Earthquake Engineering*, Vol. 7, No. 3, (2003), 347-372.
5. Kayen, R.E. and Mitchel, J.K., "Assessment of Liquefaction Potential during Earthquakes by Arias Intensity", *Journal of Geotechnical and Geoinvironmental Engineering*, Vol. 123, (1997), 1162-1174.
6. Dobry, R., Idriss, I.M. and Ng, E., "Duration Characteristics of Horizontal Component of Strong-Motion Earthquake Records", *Bulletin of the Seismological Society of America*, Vol. 68, (1978), 1487-1520.
7. Wilson, R.C. and Keefer, D.K., "Predicting a Real Limits of Earthquake-Induced Land Sliding", US Geological Survey, CA, U.S.A., Vol. 1360, (1985), 317-345.
8. Arias, A., "A Measure of Earthquake Intensity", In Hansen, R.J. (ED.), *Seismic Design for Nuclear Power Plants*, MIT Press, Cambridge, MA, U.S.A., (1970), 438-483.
9. Harp, E.L. and Wilson, R.C., "Shaking Intensity Thresholds for Rock Falls and Slides: Evidence from 1987 Whittier Narrows and Superstition Hills Earthquake Strong-Motion Records", *Bulletin of the Seismological Society of America*, Vol. 85, (1995), 1739-1757.
10. Cabanas, L., Benito, B. and Herfaiz, M., "An Approach to the Measurement of the Potential Structural of Earthquake Ground Motion", *Earthquake Engineering and Structural Dynamic*, Vol. 26, (1977), 79-92.
11. Seed, H.B. and Idriss, I.M., "Simplified Procedure for Evaluating Soil Liquefaction Potential", *Journal of Soil Mechanic and Foundation*, Vol. 97, No. 9, (1971), 1249-1273.
12. Liang, L., Figueroa, L. and Saada, A.S., "Liquefaction under Random Loading: unit Energy Approach", *Journal of Geotechnical Engineering*, Vol. 121, No. 11, (1995), 776-781.
13. Jafari, M.K., "Complementary Microzonation Studies for South of Tehran", International Institute of Earthquake Engineering and Seismology (IIEES), Tehran, Iran, (in Persian), (2003), 2-9.
14. Jafari, M.K., "Site Affects Microzonation for North of Tehran", International Institute of Earthquake Engineering and Seismology (IIEES), Tehran, Iran, (in Persian), (2003), 16-25.
15. Berberian, M., Ghoreishi, M., Ravesh, B.A. and Ashjaei, A.M., "Seismotectonic and Earthquake Fault Hazard Investigations in the Tehran Region", Geological Survey of Iran, Tehran, Iran, Report No. 56, (in Persian), (1983).
16. Nowroozi, A., "Empirical Relations between Magnitude and Fault Parameters for Earthquakes in Iran", *Bulletin of the Seismological Society of America*, Vol. 75, No. 5, (1985), 1327-1338.
17. Ghodrati Amiri, G., Mahmoodi, H. and Razavian Amrei, S.A., "Seismic Hazard Assessment of Tehran Based on Arias Intensity Parameter", *Int. Seismic Engineering Conference Commemorating the 1908 Messina and Reggio Calabria Earthquake (MERCEA08)*, Reggio Calabria, Italy, (2008), 270-276.
18. Moinfar, A., Mahdavian, A. and Maleki, E., "Historical and Instrumental Earthquake Data Collection of Iran", Mahab Ghods Consultant Engineers, Internal Report (in Persian), Tehran, Iran, (1994).
19. Gardner, J.K. and Knopoff, L., "Is the Sequence of Earthquake in Southern California, with Aftershocks removed, Poissonian?", *Bulletin of the Seismological Society of America*, Vol. 64, No. 5, (1974), 1363-1367.
20. IRCOLD, "Iranian Committee of Large Dams "Relationship between  $M_s$  and  $m_b$ ", Internal Report (in Persian), Tehran, Iran, (1994).
21. Gutenberg, B. and Richter, C.F., "Seismicity of the Earth and Associated Phenomena", Princeton University Press, NJ, U.S.A., (1954).
22. Kijko, A., "Statistical Estimation of Maximum Regional Earthquake Magnitude  $M_{max}$ ", Workshop of Seismicity Modeling in Seismic Hazard Mapping, Poljce, Slovenia, (May 22-24, 2000), 1985.
23. Tavakoli, B., "Major Seismotectonic Provinces of Iran", International Institute of Earthquake Engineering and Seismology (IIEES), (in Persian), Tehran, Iran, (1996).
24. Ghodrati Amiri, G., Motamed, R., Hashemi, R. and Nouri, H., "Evaluating the Seismicity Parameters of Tehran, Iran", *Journal of Geotechnical Engineering (Proceeding of the Institution of Civil Engineers)*, Vol. 159, No. GE4, (2006), 275-283.
25. Bender, B. and Perkins, D.M., "SEISRISK III, a Computer Program for Seismic Hazard Estimation", US Geological Survey, Bloomington, IN, U.S.A., (1987).
26. M.P.O., "Instruction for Seismic Rehabilitation of Existing Building, Standard No 360", Management and Planning Organization, Tehran, Iran, (in Persian), (2007).
27. MahdaviFar, M., Jafari, M.K. and Zolfaghari, M.R., "The Attenuation of Arias Intensity in Alborz and Central Iran", *Proceeding of the Fifth International Conference on Seismology and Earthquake Engineering*, Tehran, Iran, No. 376, (2007).
28. Travasarou, T., BRey, J.D. and Abrahamson, N.A., "Empirical Attenuation Relationship for Arias Intensity", *Earthquake Engineering and Structural Dynamic*, Vol. 32, (2003), 1133-1155.
29. Tselentis, G.A., Danciu, L. and Gkika, F., "Empirical Arias Intensity Attenuation Relationships for the Seismic Hazard Analysis of Greece", *Earthquake Resistant Engineering Structures V, The Built Environment, University of Thessaloniki, Greece*, Vol.81, (2005), 33-42.

30. Tavakoli, B., "The Basics of Seismic Hazard Analysis", International Institute of Earthquake Engineering and Seismology (IIEES), Tehran, Iran, in Persian, (1994), 1-43.
31. Wells, D.L. and Coppersmith, K.J., "New Empirical Relationships among Magnitude, Rupture Length, Rupture Width, Rupture Area and Surface Displacement", *Bulletin of the Seismological Society of America*, Vol. 84, No. 4, (1994), 974-1002.
32. Shah, H.C., Manoutchehr, M. and Zsutty, T., "Seismic Risk Analysis for California State Water Project Research", The John A. Blume Earthquake Engineering Center, Stanford University, Stanford, CA, U.S.A., Report No. 22, (1976).
33. Green, A.R. and Hall, W.J., "An Overview of Selected Seismic Hazard Analysis Methodologies", A Report on a Research Project, Department of Civil Engineering, University of Illinois at Urbana-Champaign, Champaign, IL, U.S.A., (1994).
34. Shah, H.C. and Dong, W.M., "A Re-evaluation of the Current Seismic Hazard Assessment Methodologies", *Proceedings of the 8<sup>th</sup> World Conference on Earthquake Engineering*, San Francisco, U.S.A., (1984), 247-254.
35. EERI Committee on Seismic Risk, "The Basics of Seismic Risk Analysis", *Earthquake Spectra*, Vol. 5, No. 4, (1989), 675-702.
36. Reiter, L., "Earthquake Hazard Analysis: Issues and Insights", Columbia University Press, New York, U.S.A., (1990).
37. McGuire, R.K., "Probabilistic Seismic Hazard Analysis and Design Earthquakes: Closing the Loop", *Bulletin of the Seismological Society of America*, Vol. 85, No. 5, (1995), 181-200.
38. Abdalla J.A., Mohamedzein, Y.E-A. and Abdel W.A., "Probabilistic Seismic Hazard Assessment of Sudan and its Vicinity", *Earthquake Spectra*, Vol. 17, No. 3, (2001), 399-415.